Exploring the efficacy of E7449 Anti-cancer Agent binding to PARP1: a molecular dynamics simulation approach

Hamed Esmaeil Lashgarian[1], Vahideh Assadollahi[2*], Masumeh Jalalvand[3*], Hamidreza Khodadadi[4], Leila Abkhooie[3], Amirmasoud Jalalvand[5], Mansoreh Abdolhosseini[6]

1. Associate Professor, Department of Medical Biotechnology, Faculty of Medicine, Lorestan University
2. Assistant Professor, Department of Tissue Engineering & Applied Cell Sciences, School of Advanced Technologies, Shahrekord University of Medical Sciences, Shahrekord, Iran.
3. Assistant Professor, Department of Medical Biotechnology, Faculty of Medicine, Lorestan University of Medical Sciences, Khorramabad, Iran.
4. Assistant Professor, Hepatitis Research Center, Department of Medical Biotechnology, Faculty of Medicine, Lorestan University of Medical Sciences, Khorramabad, Iran
5. Department of Medical Biotechnology, school of advanced Medical Sciences and Technologies, Shiraz University of Medical Sciences, Shiraz, Iran.
6. Department of Molecular Medicine, School of Advanced Technologies in Medicine, Tehran University of Medical Sciences, Tehran, Iran.

Corresponding author: Vahideh Assadollahi, Email: anna.assadollahi@gmail.com
Co-corresponding author: Masumeh Jalalvand, Email: masumehjalalvand@gmail.com

ABSTRACT

Poly polymerase 1, a protein of the PARP family, is involved in the cellular processes of DNA damage repair and apoptosis. Disabilities within the work of this protein can lead to distinctive illnesses, including cancer. E7449 is a novel PARP inhibitor with great potential as a cancer therapeutic. The point of this study is to investigate the interaction between E7449 and the PARP1 protein. In this study, a model of PARP1 protein was created with Modeller 9.16 software. First, we chose a model of PARP1 with a high degree of similarity to the Protein Data Bank, and introduction of this model into the simulation stage was based on energy. Simulation of its molecular dynamics was performed via GROMACS, after which its connection areas with E7449 were ascertained by AutoDock 4.2 software. The stability of the root mean square deviation diagram and energy indicated that the three-dimensional structural model was stable and closely approximated natural PARP1. Docking studies also showed that this protein has an attachment site for E7449. Given the biological importance of PARP1, the findings of this study suggest that its simulation in an in silico *environment could be used to design inhibitory ligands for eventual therapeutic purposes.*

Keywords: *Molecular dynamics simulation, PARP1, E7449, DNA repair*

1. INTRODUCTION

Poly (ADP-ribose) polymerases (PARPs) are enzymes involved in several reparative activities in response to DNA damage. PARPs constitute a different bunch of 18 proteins coded by different genes, all of them have a preserved catalytic domain. Among these, PARP1, the founding member, and PARP2 are the select proteins whose catalytic capacities are specifically activated by DNA strand breaks (1). These specific isoforms are involved in cell proliferation and death, preservation of chromatin structure, transcription, replication, recombination, cancer cell repair, and DNA repair processes (2). It has been detailed that radiation and agents that cause DNA damage increase PARPs activity. Some cellular substrates for PARP have been determined, most of which are nuclear proteins involved in nucleic acid metabolism. PARP1 is the first and most well-described member of the PARP family, while PARP2 has been described as expressing a catalytic domain with 69% similarity compared to PARP1 (1, 3, 4). PARP1 and PARP2 also cooperate with proteins involved in cell division and the mitotic spindle checkpoint (5-7). Hyperactivation of the PARP pathway may selectively cause the death of cancer cells, and hence cancer patients may be treated with small molecule inhibitors of PARPs as chemotherapy sensitizers (4, 8). New mechanisms known for cellular resistance to PARP inhibitors may indicate how these drugs can be best used in the clinic (9).

Structurally, PARP1 composed of four distinct functional domains: an (N)-terminal DNA-binding domain (DBD); an automodification domain (AD) containing a BRCT motif, which constitutes the main protein coupled with different nuclear partners; a tryptophan-glycine–arginine-rich (WGR) domain; and a carboxy catalytic domain (C)-terminal (CAT) (10, 11). The DBD is equipped with two zinc fingers (ZF1 and ZF2) that facilitate the binding of PARP1 to DNA single-strand breaks (SSBs) and DNA double-strand breaks (DSBs), thereby enhancing enzymatic activity (8, 12). When bound in response to DNA damage, PARP1 requires NAD+ to generate a radiating polymer of ADP ribose on different nuclear protein acceptors, typically associated with chromatin or self-bound in an auto modification response. The majority of these structural elements are illustrated in Figure 1.

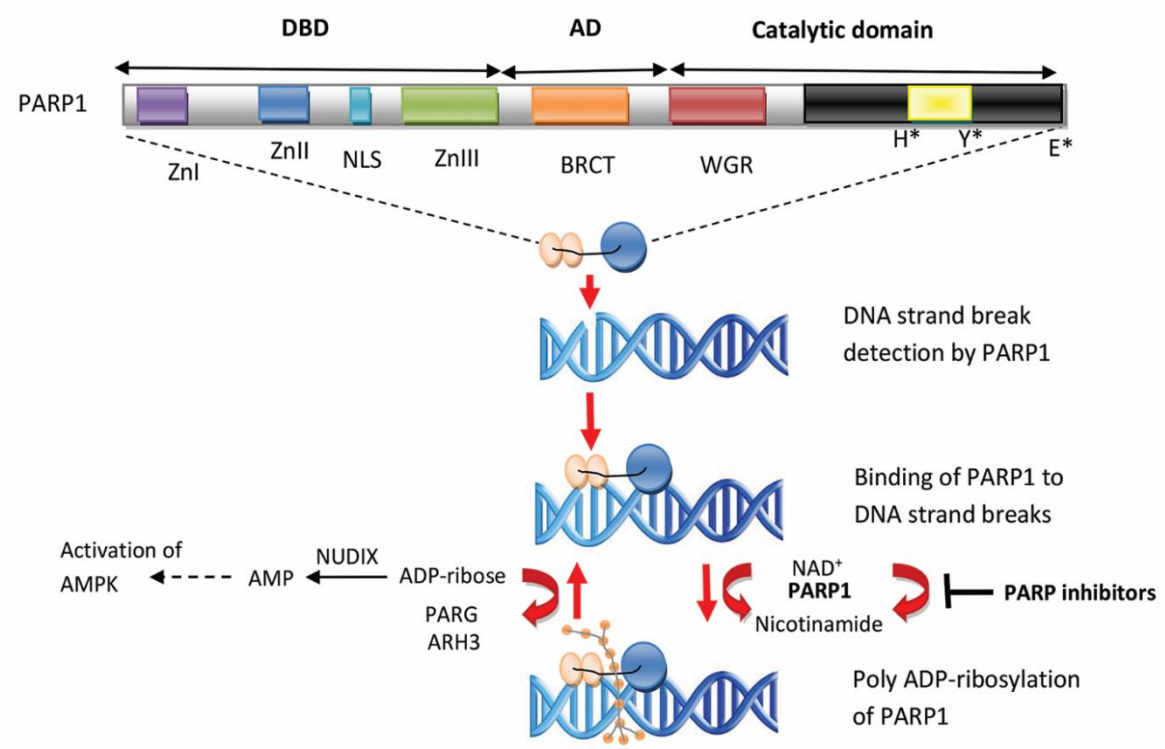

Fig1. Structure of PARP1 with its domains and mechanism of action of its inhibitors.

Heteromodification and auto modification have the same role and contribute positively to the survival of damaged cells in the proliferating stage (13). It has been shown that the short patch repair (SPR; replaces one nucleotide) and the long patch repair (LPR; resynthesis of 2−6 nucleotides) pathways, which are proliferating cell nuclear antigen (PCNA)-dependent, were mostly affected in PARP1-deficient cells (14).

PARP1 enzyme inhibitors are a new class of anticancer drugs that specifically kill cancer cells by targeting defects in homologous recombination (HR) repair. Several of these drugs are approved for the treatment of human malignancies or are currently undergoing clinical investigation. Olaparib (AZD-2281), veliparib (ABT-888), and rucaparib (AG-014699, PF-01367338) have been used as treatments for ovarian cancer, breast cancer, prostate cancer, pancreatic cancer, and some solid tumors (15). The novel anticancer drug E7449 (also called 2X-121) is an oral medicine with the ability to permeate the blood-brain barrier (BBB) and is a potent small-molecule inhibitor of PARP1 and PARP2. In preclinical studies, E7449 has been demonstrated to augment the antitumor activity of chemotherapy and radiotherapy and has acted as a single agent in BRCA-deficient and various other tumors. The protein known as Breast Cancer Type 1 susceptibility protein is a protein encoded by the BRCA gene in humans. Stage 1 research on E7449 as an antitumor agent is in progress to determine the maximum tolerated dose (MTD), safety, pharmacokinetics, pharmacodynamics, pilot activity, and investigative biomarker analysis. Moreover, E7449 demonstrates inhibitory effects on Tankyrase1 (TNKS1) and TNKS2. TNKS serves as a crucial modulator of the Wnt/β-catenin signaling pathway, promoting the proliferation of malignant cells; hence, targeting TNKS could potentially serve as a viable approach in

cancer treatment. TNKS1 and TNKS2 exhibit sequence homologies with PARP1 in their PARP catalytic domain; nevertheless, there are significant disparities between the two proteins. Specifically, TNKS1 and TNKS2 contain frequent ankyrin repeat clusters for the detection and connection of substrate proteins and a sterile α-motif that acts as a middle protein-protein interaction and for self-oligomerization (16). Prevention of DNA repair by PARP1/2 inhibition in tumor cells sensitive to radiotherapy and cytotoxic compoinds provides the rationale for administering PARP inhibitors as anticancer agents in combined therapy (17). E7449-mediated tankyrase inhibition leads to a significant increase in axin2 while reducing active and total β-catenin in human colon cancer. E7449 shows antitumor activity in several BRCA-deficient xenograft models as well as other in vivo models. A clinical trial of phase 1 for single-agent E7449 in patients with advanced malignancies was also promising (18).

Molecular docking is a computational technique utilized for predict interactions between macromolecules at the atomic level. Applications of molecular docking include the prediction of ligand–receptor interactions and drug design. In many cases, AutoDock software can be used to detect and identify new drugs (19). In general, the docking process consists of two main steps. Firstly, the sampling step involves the creation of different conformations of a ligand and examining their orientations towards the active site of the protein. During the sampling step, the docking algorithm places various versions of the ligand in the receiver's active position and ranks them according to the scoring function (20). The second scoring stage then becomes an important component in docking programs. The scoring stage is used to select the best combination or formulation of a ligand as a measure of the binding affinity of the ligand to the receptor. This function enables the docking algorithm to rapidly determine the amount of interaction between the ligand and receptor.

The role of PARP1 in various tumors remains obscure. Improving drug efficacy and reducing associated toxicity is a major concern in the development of new therapeutics or repurposing the current drugs for new targets or in combinational therapy. Although FDA-approved inhibitors such as olaparib are clinically available for PARP1, here we examine the effects of E7449 on PARP1 as a new inhibitor in an attempt to improve the effectiveness of this treatment. In this study, we assess the interaction of the anticancer drug E7449 with the PARP1 protein precisely determine where E7449 attaches to PARP1, and elucidate the important amino acids involved in this connection to shed light on the molecular mechanism of this drug.

2. Methods

2.1. Structures used

Normal PARP structure with PdbID = 4PJT.pdb was extracted from the PDB Data Bank www.rcsb.org/ PDB ID: 4zau). The following residues were not present in the structure: GLY 723, SER 724, SER 725, GLY 745, MET 746, LYS 747, GLY 781, SER 782, ASP 783, ASP 784, and SER 785. The missing residues were added to the structure and 100 structures were created using Modeller Software Version 9.16. According to PdbID = 4PJT, we selected the best models based on energy. Molecule energy minimization was conducted in a vacuum

using GROMACS. This step is crucial to eliminate false van der Waals interactions and better conformational status. The structural topology and protein sequence are shown in Figure 2.

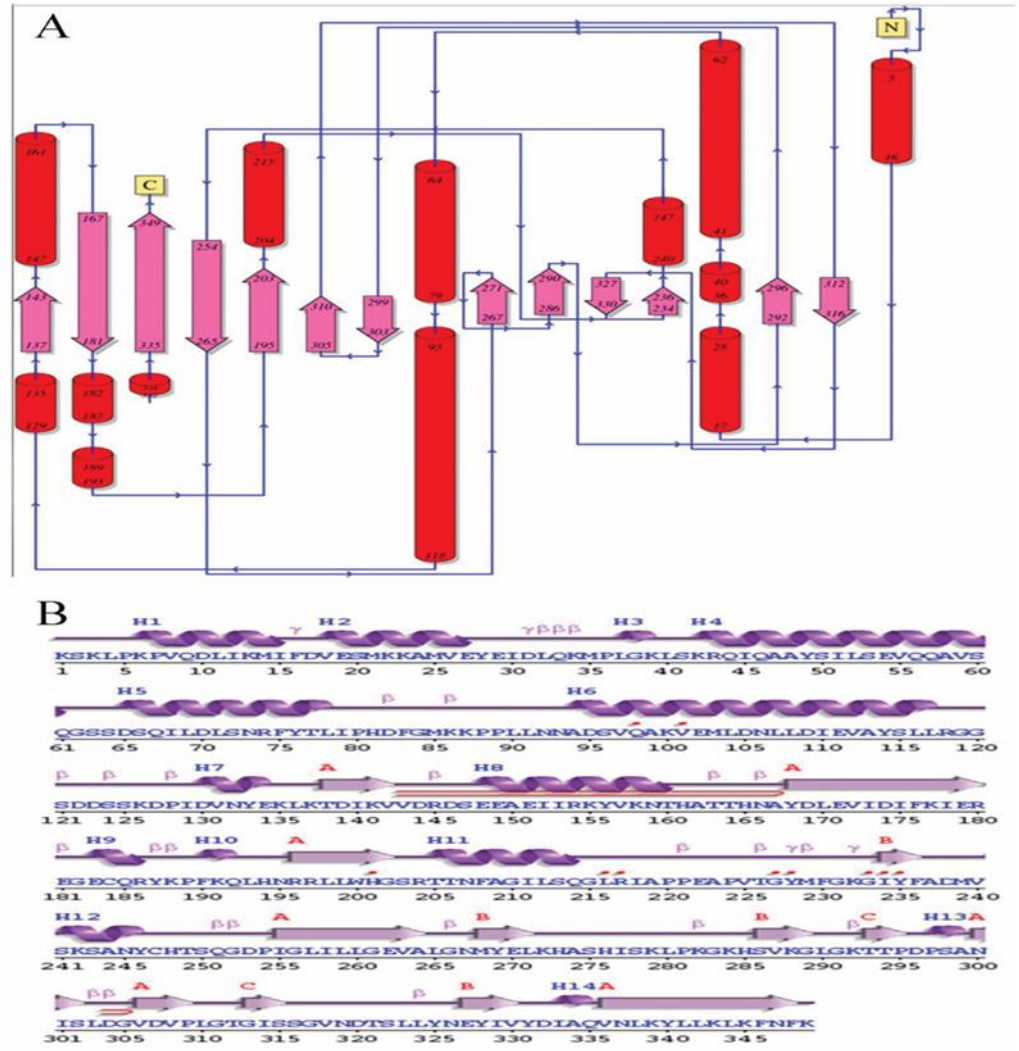

Fig 2. A) Structural topology and B) protein sequence of PARP-1

The structure of the E7449 drug was extracted from the ChemSpider Data Bank with ChemSpider ID 35308197.

2.2. Docking

Docking operations of E7449 and PARP1 were separately performed using AutoDock software version 4.2. Docking was performed by the Lamarckian genetic algorithm (LGA) 1000 times for each structure. In all dockings, a rigid PARP1 structure and a flexible drug were considered. The flexibility of the drug and the number of atoms and bonds allowed to rotate were defined for the software at the highest levels. After docking,

the best of the thousands of obtained complexes were selected for the PARP1 structure based on binding energy, constant connection, and cluster abundance. At the end of this stage, the best structure was obtained for further investigation.

2.3. Dynamic molecular simulations

PARP1 structures obtained from docking following by a dynamic molecular simulations which placed for 30 nanoseconds as previously described (21-23). Before the simulations, the E7449 drug was also prepared for detection by the force field of GROMACS. For this, hydrogen was added to the drug using Chimera software. Then, GAFF topologies were produced for the drug by AmberTools software package version 16, and the Antechamber and PARMCHECK software. The partial charges were calculated by the restrained electrostatic potential method. Finally, GAFF topologies were changed to the appropriate format to fit GROMACS by the ACPYPE tool. Then, dynamic molecular simulations using GROMACS software were performed on the CO-1686 and PARP1 structures for approximately 30 nanoseconds each. Van der Waals forces were managed with a cutoff of 10 Å. The technique of particle mesh Ewald was implemented utilizing a 10 Å cut-off threshold. The frequency was set at 10 during simulation to update the neighbor list. Also, the cutoff value was adjusted for these items as follows: short-range neighbor list cutoff = 1.2 nm, short-range electrostatic cutoff = 1.2 nm, and short-range Van der Waals cutoff = 1.2 nm.

To calculate the total load, we used the protonation state complex of the GROMACS software package. Sodium and potassium ions were used to balance the system. Each simulation consisted of four stages. In the initial stages, the system underwent minimization by utilizing steepest descent and conjugate gradient algorithms. Subsequently, in the second equilibration step, the heavy atom motion was constrained by a force constant of 1000 kJ/mol nm, while the solvents, ions, and non-heavy atoms were permitted to move. The operation was arranged by the NVT and NPT ensemble for 100 picoseconds. The system temperature was set at 298 Kelvin degrees and the pressure on 1 atmosphere and speed increased according to temperature increases by Maxwell-Boltzmann distribution. Temperature coupling was set at 0.1 picoseconds and the pressure coupling at 2 picoseconds. During equilibration for the thermostat and barostat, we used the Berendsen algorithm and all links were considered constrained by the LINCS algorithm. In the last 30 nanoseconds, a molecular dynamics simulation was performed using the NPT ensemble, where the Nosé-Hoover thermostat and Parrinello-Rahman barostat were utilized to maintain constant temperature and pressure conditions.

3. Results and Discussion

3.1 Root-mean-square deviation (RMSD)

During a simulation, the root-mean-square deviation (RMSD) is one of the important indicators in the trajectory of models. RMSD shows the extent of deviation of the position of particles in relation to the reference position at each point in time. RMSD is calculated to study atomic fluctuations of proteins and ligands during Molecular Dynamics (MD) simulation. In the equilibrium state, the extent of changes in RMSD of the carbon

alpha should be less than 2 Å. The larger the RMSD for one or a group of atoms during simulation, the greater the extent of its structural changes during the simulation. Thus, the slope of RMSD represents the stability of the model during the simulation. The closer the slope to zero, the more stable the simulated model. On the other hand, as the slope grows gradually or finds major fluctuations, the model will be less stable (24). The RMSD between structures generated during the simulation of temporal dynamics serves as a suitable measure for verifying the stability of a dynamic molecular simulation. Hence, alterations in the RMSD values of the primary chain atoms (specifically, carbon alpha) of the PARP1 molecule were computed and isolated concerning the initial structure over a simulation period of 30 nanoseconds (Figure 3). As seen in Figure 2, after approximately 5 nanoseconds, the structure of PARP1 became relatively stable and stabilized after 15 nanoseconds. The chart clearly demonstrates that the performed stimulations had satisfactory stability and the structure produced in 30 nanoseconds did not show any significant deviation. An analysis was also conducted on the variations in potential energy, pressure, temperature, and density in PARP1 during the equilibration phase to ensure the stability of the simulations. The finding showed that, in all of these cases, there was the PARP1 structures exhibited acceptable stability.

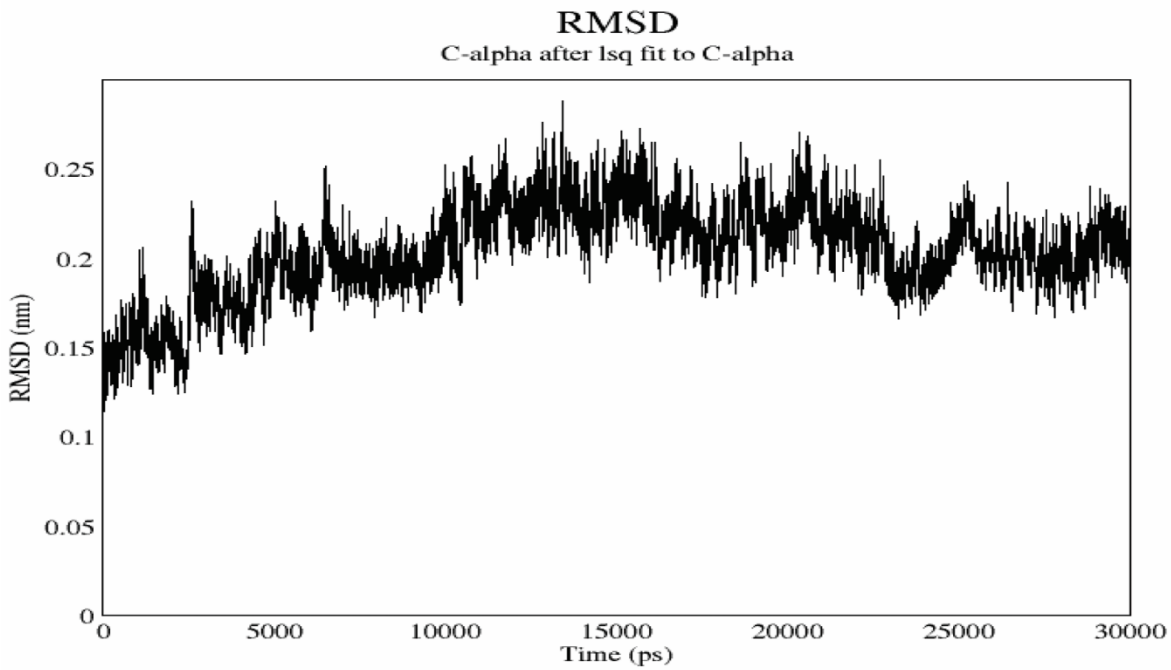

Fig 3. RMSD changes for PRP-1 within 30 nanoseconds.

3.2 Root-mean-square fluctuation (RMSF)

The motion of alpha carbon atoms within the structure provides ample data to discern significant protein movements, reflecting overall structural dynamics. Thus, the root-mean-square fluctuation (RMSF) of an alpha carbon was considered to evaluate structural movement and flexibility. In this section, we investigated the flexibility of PARP1. The maximum structural fluctuation occurred in the residue area, between 100 and 200 (Figure 4).

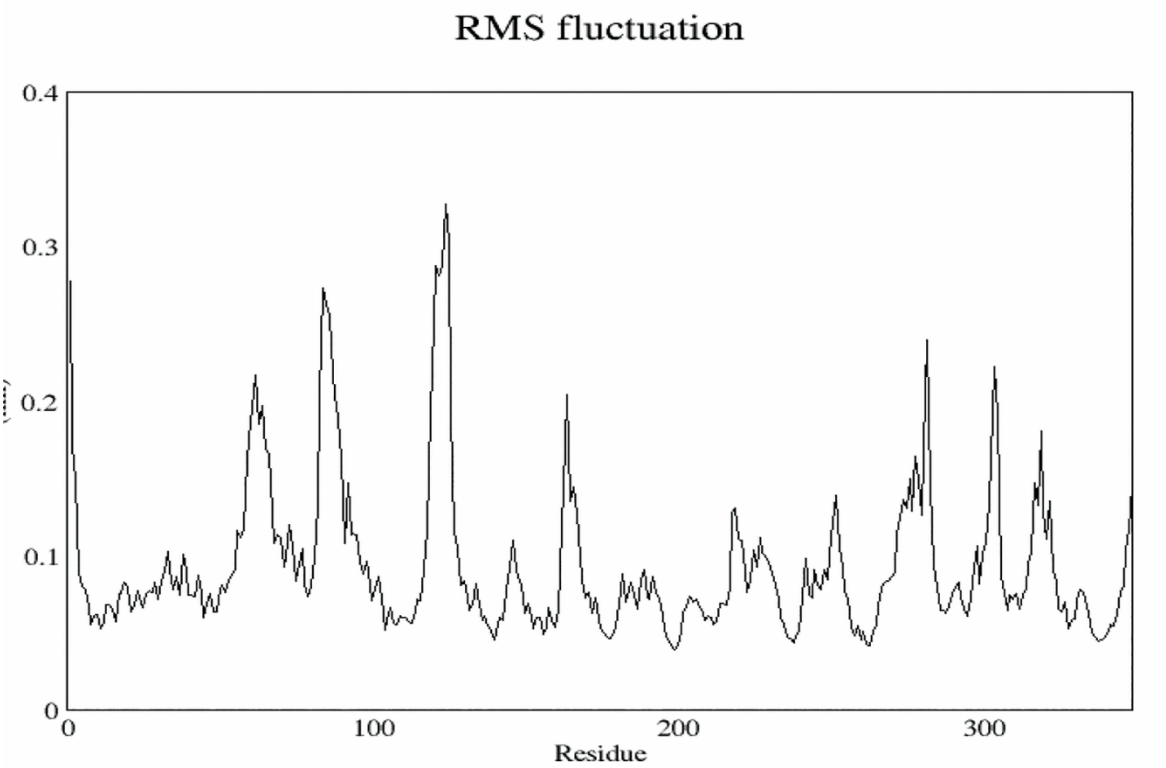

Fig 4. RMSF changes for PARP-1 within 30 nanoseconds.

3.3 Radius of gyration

In addition, the radius of the gyration is a significant parameter that indicates the amount of folding of a protein and can be utilized to assess alterations in protein conformation. A stable gyration radius indicates well-folded protein structure, which provides useful information about the distribution of proteins in a spherical shape. We calculated the changes in the gyration radius of PARP1 during 30 nanoseconds of dynamic molecular simulations (Fig. 5). As observed in Figure 5, the gyration radius for PARP1 during this time had a fixed mean, indicating that the structure of PARP1 was well-folded and stable.

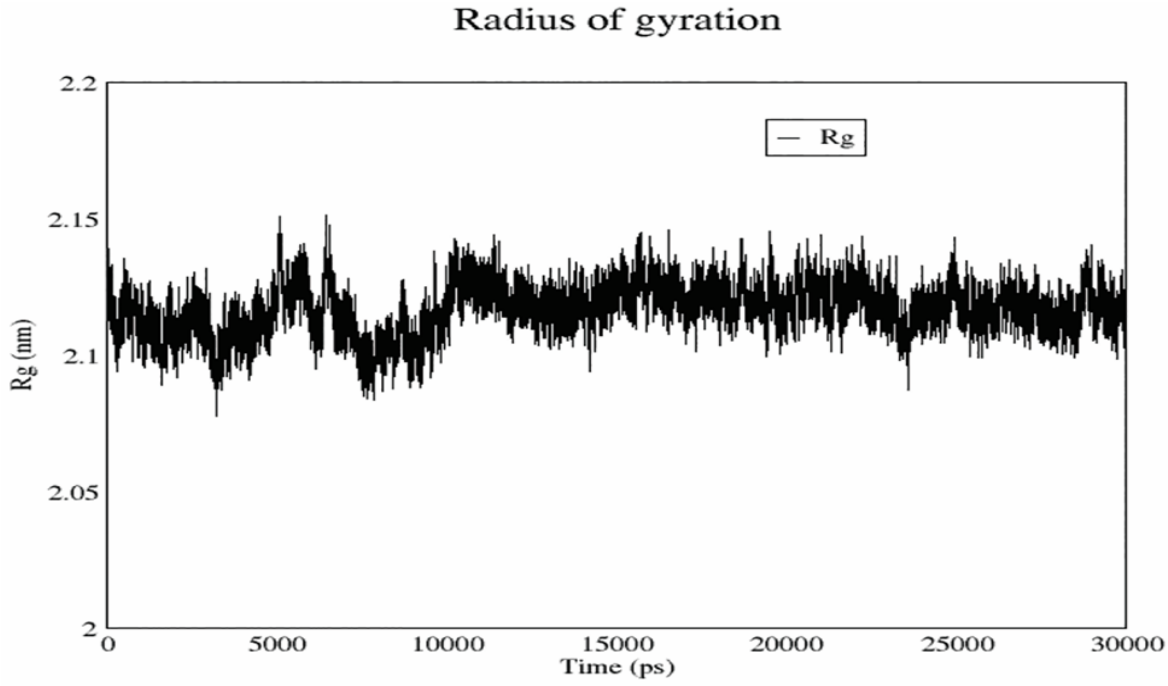

Fig 5. The changes in the gyration radius for PARP-1 within 30 nanoseconds.

3.4 Binding energy

To calculate the binding energy, we used the molecular mechanics Poisson-Boltzmann surface area (MM-PBSA) method. The energy of the tendency of compounds to bind to the target protein was calculated as kcal/mol, where lower energies suggest an enhanced tendency of the ligand to attach to the site and vice versa. The binding energy was calculated through the following equation:
The MM-PBSA equation is summarized as follows:

ΔGbind = G complex – G free-Protein - G free-ligand

G = Egas +G solvation -TS,
Gsolvation = GPB +Gsur,
Gsur = ɣA +b.

The energy in the Egas gaseous state is obtained by the following equation:

Egas=Ebond+Eangle+Etors+Evdw+Eelec

The terms Ebond, Eangle, and Etors arise from covalent, bending, and torsional bond interactions, respectively. Evdv and Eelec result from Van der Waals and electrostatic interactions. Note that the total Egas energy is obtained through the same force field, which had been used to calculate the molecular dynamics. Gsolvation represents the free energy of solvation and TS is the entropy distribution of the dissolved compound. Gsolvation consists of two parts: polar solvation energy (GPB) and non-polar solvation energy GPB (Gsur), which is an outcome of the electrostatic potential between the solvent and solute. APBS software is used to solve numerical equations associated with the Poisson-Boltzmann equation. The non-polar or superficial

solvation (Gsur) consists of three factors: an available area (A), and two experimental factors γ=0.0072 Kcal/(mol.Å2) and b=0.

To calculate the free energy using this method, first we separately investigated the energy values related to the protein and the ligand. Then, during the simulation operation, their complex energy was examined (Table 1).

Table1. Summary of connector energies for PARP-1 and E7449

	Energy type	Calculated energy(kJ/mol)	
1	van der Waal energy	-153.351 +/- 10.076	-159.447 +/- 9.742
2	Electrostatic energy	-111.052 +/- 18.904	8.228 +/- 22.135
3	Polar solvation energy	130.626 +/- 18.808	187.729 +/- 25.974
4	SASA energy	-14.305 +/- 0.748	-15.151 +/- 0.950
5	Binding energy (kJ/mol)	-148.082 +/- 15.784	21.359 +/- 14.078

From among the design compounds, we chose the best design based on the attachment energy, attachment constant, and attachment cluster frequency (Table 2).

Table2. Properties of the bests design compounds (structures)

clusters	complexes	Binding energy
1	99	**-9.74**
2	72	**-9.41**
3	11	**-8.95**
4	13	**-8.85**

Out of the four selected compounds, cluster 1 with 99 complexes and an attachment energy of -9.74 was chosen as the most optimal compound. The general characteristics of cluster 1 are reported in (Table 3).

Table3. General characteristics of cluster 1

Binding Energy	-9.74
kI	72.35nM
Intermolecular Energy	-10.34
Internal Energy	-0.23
Torsional Energy	0.6
Unbound Extended Energy	-0.23
Cluster RMS	0
Ref RMS	127.93

To better understand the attachment site as well as the manner of ligation to this site, the interaction between E7449 and PARP1 was tested by LigPlo software and represented as two-dimensional. The catalytic residue involved with the PARP1-E7449 compound included Arg217, which is involved in the hydrogen bond, as well as Leu216, His201, I1234, Try235, Gly227, Gln98, and Val101, which are involved in unbonded reactions (Figure 6).

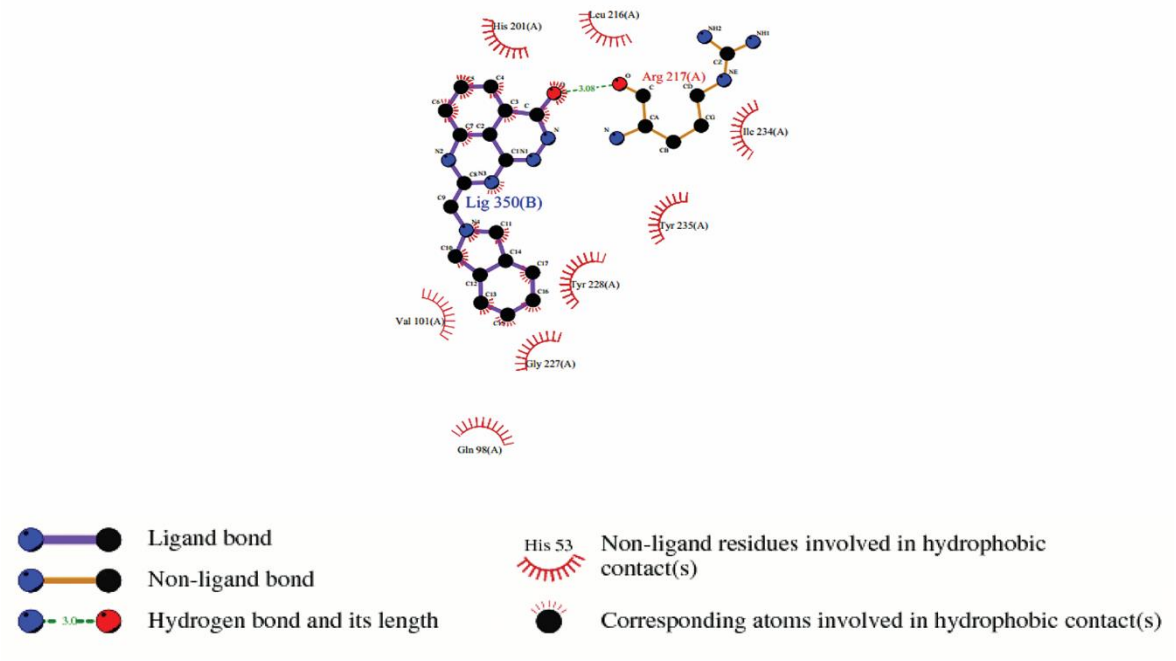

Fig 6. Interaction between PARP-1 and E7449 by LigPlo.

The design and development of drugs is a costly, time-consuming process that requires extensive laboratory assessments before a drug can reach the market. Accordingly, developing methods that enable millions of compounds to be screened within a shorter time and with a decreased cost is crucial. Today, in silico methods are considered one of the least expensive and most rapid solutions for assessing promising compounds or drugs (25).

4. Conclusion

In the present research, we investigated the possible site of the attachment between the E7449 anticancer drug and the PARP1 protein. Inhibiting PARP1 in cancers with deficiencies in homologous recombination (HR) repair, such as those with mutations in BRCA1 or BRCA2, results in effective cell death via synthetic lethality. Furthermore, the impaired DNA repair by the inhibition of PARP1 and PARP2 enhances the susceptibility of cancerous cells to radiotherapy and cytotoxic agents that disrupt DNA integrity. This emphasizes the justification for using PARP inhibitors as anticancer agents in combination therapy. Each PARP protein consists of a catalytic domain with an ADP-ribosyl transferase domain (ART) that contains the residue of a conserved glutamic acid. The catalytic domain in the PARP family of proteins plays a very significant role in the function of these proteins as well as the interaction between these proteins and other proteins (26, 27). The catalytic domain in the PARP1 protein lies in the C-terminal region with 489 amino acids beginning from amino acid number 525 and continuing until number 1014. The active sites of the PARP1 protein are also located in this region. The N-terminal domain of this protein contains ZF motifs attached to a DNA molecule,

and it is involved in protein-protein interactions. Impairment in the activity of the PARP1 protein, as one of the factors involved in cellular processes such as DNA repair and apoptosis, leads to diseases such as cancer (28).

E7449, identified as a robust inhibitor of PARP1 and PARP2, is recognized by its alternative nomenclature TNKS1 and TNKS2, respectively, both serving as pivotal modulators within the canonical Wnt/β-catenin pathway. E7449 inhibits PARP enzymatic activity and additionally traps PARP1 onto damaged DNA (29, 30). In conclusion, our data showed the accuracy of the E7449 drug efficiency on PARP1 and provided proof of in silico *molecular dynamics on the interaction between this specific drug and its target.*

CONFLICT OF INTERESTS

The authors disclose no potential conflict of interest.

REFERENCES

1. *Morales J, Li L, Fattah FJ, Dong Y, Bey EA, Patel M, et al. Review of poly (ADP-ribose) polymerase (PARP) mechanisms of action and rationale for targeting in cancer and other diseases. Critical Reviews™ in Eukaryotic Gene Expression. 2014;24(1).*
2. *Bai P. Biology of poly (ADP-ribose) polymerases: the factotums of cell maintenance. Molecular cell. 2015;58(6):947-58.*
3. *Jain PG, Patel BD. Medicinal chemistry approaches of poly ADP-Ribose polymerase 1 (PARP1) inhibitors as anticancer agents-A recent update. European journal of medicinal chemistry. 2019;165:198-215.*
4. *Morales J. Review of poly (ADP-ribose) polymerase (PARP) mechanisms of action and rationale for targeting in cancer and other diseases. Crit Rev Eukaryot Gene Expr. 2010;1:461.*
5. *Yelamos J, Farres J, Llacuna L, Ampurdanes C, Martin-Caballero J. PARP-1 and PARP-2: New players in tumour development. American journal of cancer research. 2011;1(3):328.*
6. *Mangerich A, Bürkle A. Pleiotropic cellular functions of PARP1 in longevity and aging: genome maintenance meets inflammation. Oxidative medicine and cellular longevity. 2012;2012.*
7. *Kukolj E, Kaufmann T, Dick AE, Zeillinger R, Gerlich DW, Slade D. PARP inhibition causes premature loss of cohesion in cancer cells. Oncotarget. 2017;8(61):103931.*
8. *Ali AA, Timinszky G, Arribas-Bosacoma R, Kozlowski M, Hassa PO, Hassler M, et al. The zinc-finger domains of PARP1 cooperate to recognize DNA strand breaks. Nature structural & molecular biology. 2012;19(7):685.*
9. *Lord CJ, Ashworth A. Targeted therapy for cancer using PARP inhibitors. Current opinion in pharmacology. 2008;8(4):363-9.*
10. *Langelier M-F, Planck JL, Roy S, Pascal JM. Structural basis for DNA damage–dependent poly (ADP-ribosyl) ation by human PARP-1. Science. 2012;336(6082):728-32.*
11. *Spiegel JO, Van Houten B, Durrant JD. PARP1: Structural insights and pharmacological targets for inhibition. DNA repair. 2021;103:103125.*
12. *Wang L, Liang C, Li F, Guan D, Wu X, Fu X, et al. PARP1 in carcinomas and PARP1 inhibitors as antineoplastic drugs. International journal of molecular sciences. 2017;18(10):2111.*
13. *Amé JC, Spenlehauer C, de Murcia G. The PARP superfamily. Bioessays. 2004;26(8):882-93.*
14. *Lavrik OI, Prasad R, Sobol RW, Horton JK, Ackerman EJ, Wilson SH. Photoaffinity Labeling of Mouse Fibroblast Enzymes by a Base Excision Repair Intermediate EVIDENCE FOR THE ROLE OF POLY (ADP-RIBOSE) POLYMERASE-1 IN DNA REPAIR. Journal of Biological Chemistry. 2001;276(27):25541-8.*
15. *Kummar S, Chen A, Ji J, Zhang Y, Reid JM, Ames M, et al. Phase I study of PARP inhibitor ABT-888 in combination with topotecan in adults with refractory solid tumors and lymphomas. Cancer research. 2011;71(17):5626-34.*
16. *Lehtiö L, Chi NW, Krauss S. Tankyrases as drug targets. The FEBS journal. 2013;280(15):3576-93.*
17. *Curtin NJ, Szabo C. Therapeutic applications of PARP inhibitors: anticancer therapy and beyond. Molecular aspects of medicine. 2013;34(6):1217-56.*

18. Plummer R, Dua D, Cresti N, Drew Y, Stephens P, Foegh M, et al. First-in-human study of the PARP/tankyrase inhibitor E7449 in patients with advanced solid tumours and evaluation of a novel drug-response predictor. British Journal of Cancer. 2020:1-9.
19. Ramírez D, Caballero J. Is it reliable to use common molecular docking methods for comparing the binding affinities of enantiomer pairs for their protein target? International journal of molecular sciences. 2016;17(4):525.
20. Trott O, Olson AJ. AutoDock Vina: improving the speed and accuracy of docking with a new scoring function, efficient optimization, and multithreading. Journal of computational chemistry. 2010;31(2):455-61.
21. Rashidieh B, Valizadeh M, Assadollahi V, Ranjbar MM. Molecular dynamics simulation on the low sensitivity of mutants of NEDD-8 activating enzyme for MLN4924 inhibitor as a cancer drug. American journal of cancer research. 2015;5(11):3400.
22. Ranjbar MM, Assadolahi V, Yazdani M, Nikaein D, Rashidieh B. Virtual Dual inhibition of COX-2/5-LOX enzymes based on binding properties of alpha-amyrins, the anti-inflammatory compound as a promising anti-cancer drug. EXCLI journal. 2016;15:238.
23. Assadollahi V, Rashidieh B, Alasvand M, Abdolahi A, Lopez JA. Interaction and molecular dynamics simulation study of Osimertinib (AstraZeneca 9291) anticancer drug with the EGFR kinase domain in native protein and mutated L844V and C797S. Journal of cellular biochemistry. 2019;120(8):13046-55.
24. Carugo O, Pongor S. A normalized root-mean-spuare distance for comparing protein three-dimensional structures. Protein science. 2001;10(7):1470-3.
25. Bai Y, Watt B, Wahome PG, Mantis NJ, Robertus JD. Identification of new classes of ricin toxin inhibitors by virtual screening. Toxicon. 2010;56(4):526-34.
26. Steffen JD, Brody JR, Armen RS, Pascal JM. Structural implications for selective targeting of PARPs. Frontiers in oncology. 2013;3:301.
27. Herceg Z, Wang Z-Q. Functions of poly (ADP-ribose) polymerase (PARP) in DNA repair, genomic integrity and cell death. Mutation Research/Fundamental and Molecular Mechanisms of Mutagenesis. 2001;477(1-2):97-110.
28. Chen K-C, Sun M-F, Chen CY-C. In silico investigation of potential PARP-1 inhibitors from traditional chinese medicine. Evidence-Based Complementary and Alternative Medicine. 2014;2014.
29. McGonigle S, Chen Z, Wu J, Chang P, Kolber-Simonds D, Ackermann K, et al. E7449: A dual inhibitor of PARP1/2 and tankyrase1/2 inhibits growth of DNA repair deficient tumors and antagonizes Wnt signaling. Oncotarget. 2015;6(38):41307.
30. Ryan K, Bolaños B, Smith M, Palde PB, Cuenca PD, VanArsdale TL, et al. Dissecting the molecular determinants of clinical PARP1 inhibitor selectivity for tankyrase1. Journal of Biological Chemistry. 2021;296.